A Precoding-based PAPR Reduction Technique for UF-OFDM and Filtered-OFDM Modulations in 5G Systems

Mouna BEN MABROUK, Marwa CHAFII, Yves LOUËT and Faouzi BADER
IETR/CentraleSupélec, Campus de Rennes, 35511 Cesson-Sevigné, France
{mouna.benmabrouk, marwa.chafii, yves.louet, faouzi.bader}@centralesupelec.fr

***Abstract*—The universal filtered-orthogonal frequency division multiplexing (UF-OFDM) (also called universal filtered multicarrier (UFMC)) and the filtered-OFDM (F-OFDM) are candidates to be alternative to the OFDM modulation in the upcoming 5G systems thanks to their improved spectral occupation and resistance to the carrier frequency offset. However, like the majority of the multicarrier modulations, UF-OFDM and F-OFDM have a high peak-to-average power ratio (PAPR). This influences the operation mode of radio frequency components such as the power amplifier and the digital-to-analog converter. In this paper, a precoding-based PAPR reduction technique is proposed for both the UF-OFDM and the F-OFDM cases. A similar technique has been proposed in the literature for OFDM. The principle of this method is to transform the UF-OFDM signal to a lower order summation of single carrier signals and the F-OFDM signal to single carrier signal. The relevance of the proposed PAPR reduction technique is confirmed by simulation results. The latter show a PAPR reduction of at least 2.5 dB. Moreover, the proposed technique does not impact the bit error rate performance and lowers down the power spectral density tails at the power amplifier output.**

***Index Terms*—PAPR, UFMC, OFDM, precoding, 5G, UF-OFDM, F-OFDM, PAPR, bit error rate, power spectral density.**

I. Introduction

The potential support of the so-called Internet of Things (IoT) and the move from cell-centric to user-centric processing are two trends related to the future 5G systems [1]. To meet the requirements of these objectives, the dynamic spectrum sharing is a key technique in order to respond to their high data rate demands [2]. Hence, to make the best use of available frequency resources without creating any interference to the neighboring nodes, spectrally contained and scalable waveforms are needed.

The orthogonal frequency division multiplexing (OFDM) modulation is a multicarrier modulation (MCM) scheme that can respond to these demands in perfect situations. Indeed, when the user is perfectly synchronized both in time and frequency domain with the base station (BS), OFDM offers good performance in terms of bit error rate (BER) and resistance to the carrier frequency offset (CFO). These circumstances are energy costly as the user needs to exchange messages with the BS to ensure this synchronization. Therefore, if these conditions are not satisfied, the OFDM BER may be high. Nevertheless, the OFDM modulation suffers from high side lobes which decreases the spectral efficiency and creates adjacent channel interferences.

For these reasons, several MCM schemes have been developed these recent years as candidates for 5G systems such as the universal filtered-OFDM (UF-OFDM) technique and the Filtered-OFDM (F-OFDM). These waveforms is considered as OFDM-like modulations so that no considerable system modifications are needed [2]. Moreover, they have better performance in terms of resistance to the CFO and lower power spectral density (PSD) side lobes. However, as it is the case of all the MCMs, these modulation schemes have high peak-to-average power ratios (PAPR).

A high PAPR increases the complexity of the analog-to-digital and the digital-to-analog converters and reduces the efficiency of the power amplifier (PA). Indeed, without any pre-processing, the PA needs to be backed off far from its saturation point. This results in a very low efficiency, typically less than 10% [3]. For this reason, this work proposes a digital PAPR reduction technique to drive the signal to be amplified as close as possible to the compression region resulting in a better efficiency. Several techniques have been proposed in literature such as phase optimization [4], tone reservation [5], tone injection [6] and precoding-based techniques [7].

The precoding-based techniques seem to be promising techniques as they are linear and simple to implement without any need of side information. Also, precoding reduces the PAPR without increasing the complexity and without destroying orthogonality between subcarriers.

In this work, we propose a PAPR reduction technique for UF-OFDM and F-OFDM based on a precoding scheme. This scheme is adapted to the UF-OFDM and F-OFDM modulations and then compared to the original scheme. This comparison is performed according to three parameters: PAPR, BER and PSD at the PA output signal.

This paper is organized as follows:
In Section II, a brief presentation of the UF-OFDM systems is given. The adopted precoding scheme is detailed in Section III. Finally, the proposed technique is evaluated by means of simulation results in Section IV.

II. PAPR for UF-OFDM and F-OFDM systems

In this Section, a brief description is firstly given. Secondly, an approximation of the PAPR of a general MCM system is

ISBN 978-3-8007-4426-8

detailed. Then, the application of this approximation to the F-OFDM and UF-OFDM is performed.

A. UF-OFDM system

As illustrated in Fig. 1, in UF-OFDM, the data symbols $\{x_n\}_{n\in[\![0,N-1]\!]}$ are assigned to each subcarrier in the allocated subcarrier set, containing N subcarriers. Then, they are divided into B sub-sets. Each sub-set contains N_B consecutive subcarriers and consequently N_B data symbols. A M-point inverse discrete Fourier transform (IDFT) operation is performed for every sub-set i to transform the frequency domain signal $\{X_b^i\}_{b\in[\![(i-1)N_B,iN_B]\!]}$ into time domain. The IDFT output signal of each sub-set $\tilde{x}_m^i$ is filtered by a Chebychev filter f_i of length L to get $\{\tilde{x}_l^{f,i}\}_{l\in[\![(i-1)(L+M-1),i(L+M-1)]\!]}$.

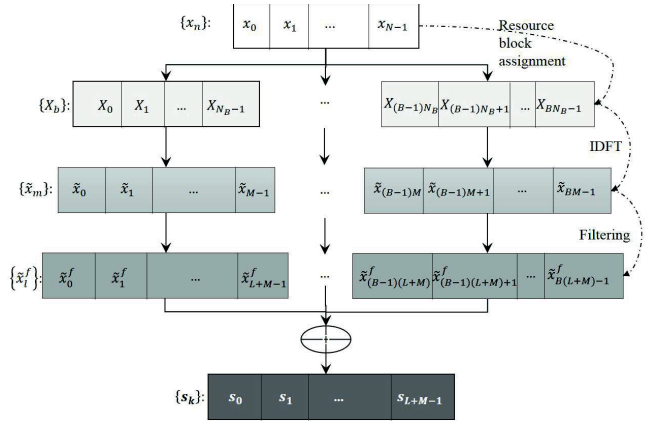

Fig. 1. Generation of the UF-OFDM signal.

B. F-OFDM systems

As depicted in Fig. 2, the F-OFDM signal is the conventional OFDM signal passed through an appropriately designed spectrum shaping filter [8]:

$$s_k = \sum_{l=0}^{M+M_g} \sum_{m=0}^{N-1} x_{m,l} f[k-lM] e^{j2\pi \frac{mk}{M}}, \tag{1}$$

where M_g is the cyclic prefix length.

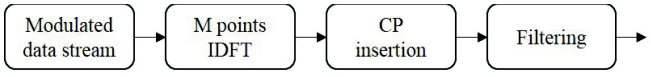

Fig. 2. Generation of the F-OFDM signal.

The spectrum shaping filter f is centered on assigned subcarriers. Its bandwidth is equal to the total frequency width of the assigned subcarriers, and its time duration is a portion of an OFDM symbol duration.

C. PAPR approximation

In a previous work [9], Chafii *et al.* developed a closed-form approximation of the PAPR CCDF for any MCMs. Let s_k a MCM transmitted signal. s_k can be written as:

$$s_k = \sum_{n\in\mathbb{Z}} \sum_{m=0}^{M-1} x_{m,n} \underbrace{g_m[k-nM]}_{g_{m,n}[k]}, \tag{2}$$

where $x_{m,n}, n \in \mathbb{Z}, m \in [\![0, M-1]\!]$ are the transmitted symbols from a complex constellation, assumed to be independent and identically distributed with zero mean and variance σ_x^2, and $g_{m,n}[k]$ is the waveform filter, as depicted in Fig. 3.

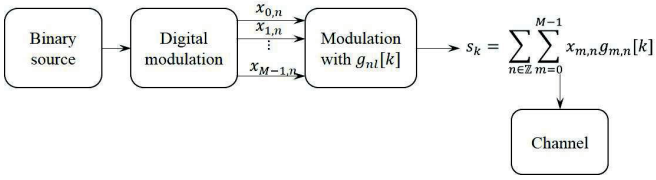

Fig. 3. Multi carrier modulations general system model.

The PAPR of a multicarrier (MC) signal is defined as:

$$PAPR = \frac{max_{k=0,\cdots,M-1}|s_k|^2}{E[|s_k|^2]}$$

where $E[\cdot]$ is the expectation value. Based on Lyapunov central limit theorem, Chafii *et al.* proved that the PAPR complementary cumulative distribution function (CCDF) of these MCMs can be approximated as follows:

$$Pr(PAPR > \gamma) \approx 1 - \prod_{k\in[\![0,NM-1]\!]} (1 - e^{-c_k\gamma}), \tag{3}$$

where

$$c_k = \frac{\sum_{n\in\mathbb{Z}} \sum_{m=0}^{M-1} |g_{m,n}[k]|^2}{N \sum_{m=0}^{M-1} |g_{m,n}[k]|^2},$$

and N is the number of MCMs frames considered in the observation and γ is the PAPR threshold. This expression is reliable when the following conditions are satisfied:

- About the input symbols: the real and imaginary parts of $(x_{m,n})_{(m\in[\![0,M-1]\!],\, n\in\mathbb{Z})}$ are independent and identically distributed.
- About the waveforms: $\{g_m\}_{m\in[\![0,M-1]\!]}$ are bounded and have a finite temporal support:

$$A := \min_{m,k} \sum_{n\in\mathbb{Z}} |g_{m,n}[k]|^2 > 0. \tag{4}$$

  In other words, the temporal support of $g_{m,n}[k]$ has to be greater or equal to the symbol block period T i.e. containing M samples.
- About the subcarrier number: The number of subcarriers is supposed to be $M \geq 8$. This is an assumption made for the validity of the central limit theorem [9].

ISBN 978-3-8007-4426-8

In other words, the temporal support of $g_{m,n}[k]$ has to be greater or equal to the symbol period T. In Fig.4, the theoretical PAPR CCDF is compared to the simulated one for both F-OFDM and UF-OFDM signals.

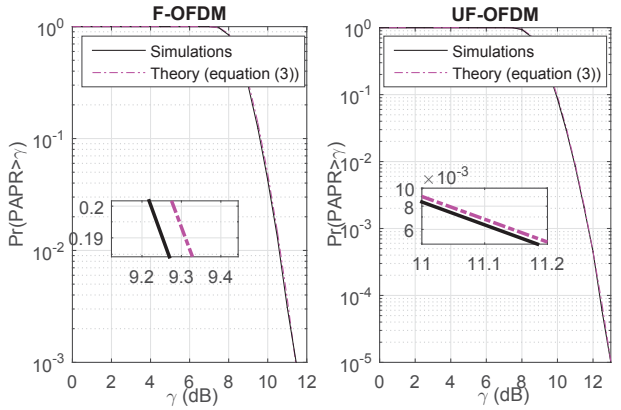

Fig. 4. Simulated and theoretical PAPR CCDF for a F-OFDM system (on the left) and an UF-OFDM system (on the right).

As mentioned previously, for any MCM waveform, a high PAPR involves that the PA operates in its linear region most of the time ensuring that the signal peaks do not exceed the PA breakdown zone. This means that the PA efficiency is averagely low. For this reason, one has to reduce the PAPR. In this work, we propose a PAPR reduction technique based on precoding. The theoretical concept and the simulation results of the proposed technique for OFDM and UF-OFDM signals are given in the following Sections.

III. Precoded UF-OFDM and F-OFDM systems

As depicted in Fig. 5, a precoding technique consists in multiplying the modulated data of each UF-OFDM block by a precoding matrix before the subset assignment IDFT block. In [7], the precoding matrix is of the same size as the allocated subcarrier vector. The dimension of the precoding matrix, denoted by $\mathbf{P}$, is, hence, $N \times N$. It is used as a spreading code and can be expressed as:

$$\mathbf{P} = \begin{bmatrix} P_{0,0} & P_{0,1} & \cdots & P_{0,N-1} \\ P_{1,0} & P_{1,1} & \cdots & P_{1,N-1} \\ \vdots & \vdots & \ddots & \vdots \\ P_{N-1,0} & P_{N-1,1} & \cdots & P_{N-1,N-1} \end{bmatrix} \quad (5)$$

To simplify the reverse precoding process, the matrix $\mathbf{P}$ has to be a unitary matrix which means that $\mathbf{P}\mathbf{P}^H = \mathbf{I}_N$. Also, as the precoding is performed before the IDFT, it should contain a signal transform to the frequency domain. Hence, we obtain:

$$\mathbf{P} = [P_{ij}]_{i,j\in[\![0,N-1]\!]} \quad (6)$$

where $P_{ij} = P_{i0}e^{-\frac{2\pi ij}{N}}$, and $P_{i0}, i \in [\![0, N-1]\!]$ are the coefficients of a mother function. In this paper, the rectangular is used as a mother function. We refer to the precoded UF-OFDM and F-OFDM using a rectangular filter respectively by DFT-UF-OFDM and DFT-F-OFDM.

The proposed precoding scheme consists in multiplying the data symbols $\{x_n\}_{n\in[\![0,N-1]\!]}$ before subdivision into sub-sets by the precoding matrix defined in (6) to obtain $\{\tilde{X}_p\}_{p\in[\![0,N-1]\!]}$. Therefore, the UF-OFDM output signal can be written as $s_k = \sum_{b=0}^{B}\sum_{m=0}^{M-1}\tilde{x}_m^b f_{k-mM}^b$ where $\tilde{x}_m^b$ is expressed as follows:

$$\tilde{x}_m^b = \sum_{p=(b-1)N_B}^{bN_B-1}\sum_{n=0}^{N-1} P_{m0}x_n e^{-j\frac{2\pi np}{N}}e^{j\frac{2\pi mp}{M}}. \quad (7)$$

Denoting $P_{m0}x_n$ by x_{mn}^b, $\tilde{x}_m^b$ can be written as:

$$\begin{aligned}\tilde{x}_m^b &= \sum_{p=(b-1)N_B}^{bN_B-1} DFT(x_{mn}^b)e^{j\frac{2\pi mp}{M}} \\ \tilde{x}_m^b &= IDFT(DFT(x_{mn}^b)) = x_{mn}^b \end{aligned} \quad (8)$$

Therfore, by replacing $\tilde{x}_m^b$ by x_{mn}^b, we obtain:

$$s_k = \sum_{b=0}^{B}\sum_{m=0}^{M-1} x_{mn}^b f_{k-mM}^b \quad (9)$$

By setting $s_k^b = \sum_{m=0}^{M-1} x_m^b f_{k-m}^b$, the UF-OFDM output signal s_k is given as:

$$s_k = \sum_{b=0}^{B} s_k^b, \quad (10)$$

where s_k^b is the single carrier (SC) signal at the output of the pulse shaping filter. Consequently, the precoded UF-OFDM signal is the summation of B SC signals. Although, UF-OFDM signal is still a multicarrier signal, the number of the subcarriers is reduced from the IDFT size M to the number of the sub-sets B. The UF-OFDM PAPR is reduced, as it is a function of a smaller number of subcarriers.

Let us now study theoretically the way the precoding matrix reduces the PAPR of a F-OFDM signal. The precoded F-OFDM signal can be written as follows:

$$s_k = \sum_{l=0}^{M+M_g}\sum_{m=0}^{N-1} X_{m,l} f[k-lM]e^{j2\pi\frac{mk}{M}}$$

where

$$X_{m,l} = \sum_{n=0}^{N-1} P_{m0}x_{n,l}e^{-j\frac{2\pi nm}{N}}$$

By setting $P_{m0}x_{n,l} = \tilde{x}_{m,l}$, we have $X_{m,l} = DFT(\tilde{x}_{m,l})$. Hence,

$$\begin{aligned} s_k &= \sum_{l=0}^{M+M_g} f[k-lM]\sum_{m=0}^{M-1} DFT(\tilde{x}_{m,l})e^{j\frac{2\pi mk}{M}} \\ &= \sum_{l=0}^{M+M_g} f[k-lM]IDFT(DFT(\tilde{x}_{m,l})) \end{aligned} \quad (11)$$

ISBN 978-3-8007-4426-8

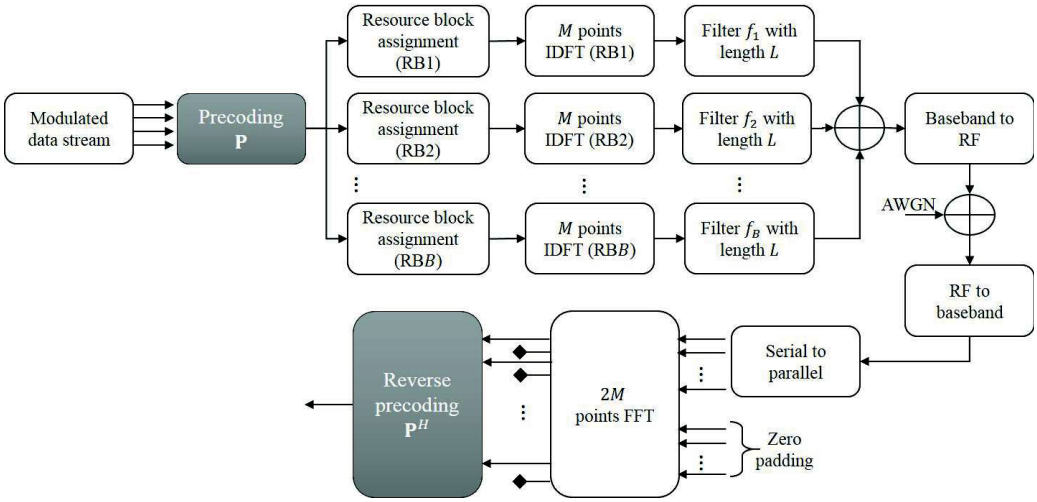

Fig. 5. Block scheme for a precoded UF-OFDM system.

So that:

$$s_k = \sum_{l=0}^{M+M_g} \tilde{x}_{m,n} f[k - lM]. \quad (12)$$

Therefore, s_k is the SC signal at the output of the pulse shaping filter and hence, the F-OFDM system becomes equivalent to a SC system.

IV. Simulation results

In this Section, a simulation-based analysis of the signal dynamics at the input and the output of the PA is provided. First, the signal dynamics of the original modulation schemes is compared to the precoded ones in terms of two signal dynamics parameters: the PAPR and the instant-to-average power ratio (IAPR). Second, the spectral shape of these signals at the PA output are presented and analyzed. Finally, the impact of the precoding procedure on the BER is studied for an additive white Gaussian noise (AWGN) channel.

A. PAPR and IAPR performance

The PAPR gives an idea about the maximum input back-off (IBO) value to be taken into account to avoid the PA breakdown. Another metric to evaluate the signal dynamics is the IAPR defined by:

$$IAPR = \frac{|s_k|^2}{E[|s_k|^2]}. \quad (13)$$

This metric corresponds to the variation of the instantaneous measured power. Therefore, thanks to a higher granularity, it provides a better appraisal of their impact on the PA. Hence, in order to better evaluate the performance of the proposed "signal dynamics" reduction technique, we consider both metrics the IAPR and the PAPR. As after precoding the F-OFDM and the UF-OFDM are equivalent to SC signals, their PAPR and IAPR might depend on the constellation choice. For this reason, let us study the impact of the constellation choice on the PAPR and IAPR reduction. For this reason, the considered UF-OFDM and F-OFDM signals in this Section have the parameters defined in TABLE I.

TABLE I
Signal parameters

DFT size: M	1024
Allocated subcarriers: N	480
Constellations	QPSK, 16-QAM, 64-QAM
UF-OFDM: Filter	Chebyshev
UF-OFDM: Filter length: L	72
UF-OFDM: Sidelobe attenuation	40 dB
UF-OFDM: Sub-set size: N_B	12
UF-OFDM: Sub-set number: B	40
F-OFDM: Filter	Truncated raised root cosine [8]

In Fig. 6 and Fig. 7, the IAPR and PAPR performance using different constellations are presented. Here, the considered mother function is the rectangular filter. It should be noted that when higher order constellations are used, such as 16-QAM and 64-QAM, the PAPR reduction performance is lower than in the QPSK case. However, the performance degradation with the proposed technique is no more significant when using 64-QAM. It shows a boundary for the PAPR and IAPR for the proposed scheme. It should be noted that with DFT-F-OFDM, we obtain as predicted better PAPR and IAPR reduction performance. Indeed, the precoding transforms the F-OFDM signal to a single carrier signal which is not the case for the UF-OFDM scheme.

B. Impact on the PA output PSD

In this part, we use the same signal characteristics for the UF-OFDM signal described in Section IV-A and the Saleh model for the PA. In Fig. 8, the value of the considered IBO is 5 dB. It can be observed, analyzing Fig. 8 that the tails of the spectrum of the OFDM, F-OFDM and UF-OFDM

ISBN 978-3-8007-4426-8

TABLE II
PSD-BASED COMPARISON BETWEEN THE UF-OFDM,THE F-OFDM, THE DFT-UF-OFDM AND THE DFT-F-OFDM.

	PA output PSD tails level frequency=15.36MHz			
	UF-OFDM	F-OFDM	DFT-UF-OFDM	DFT-F-OFDM
IBO=1 dB	-17 dB	-21	-20 dB	-24 dB
IBO=5 dB	-25 dB	-30	-30 dB	-35 dB
IBO=9 dB	-34 dB	-39	-40 dB	-47 dB

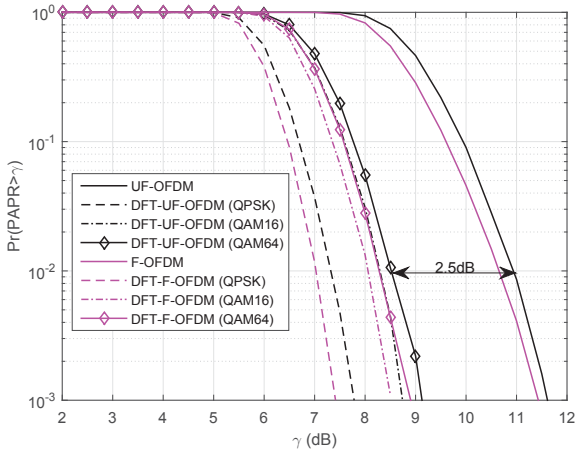

Fig. 6. PAPR performance of the rectangular-based precoded UF-OFDM and F-OFDM schemes for different constellations.

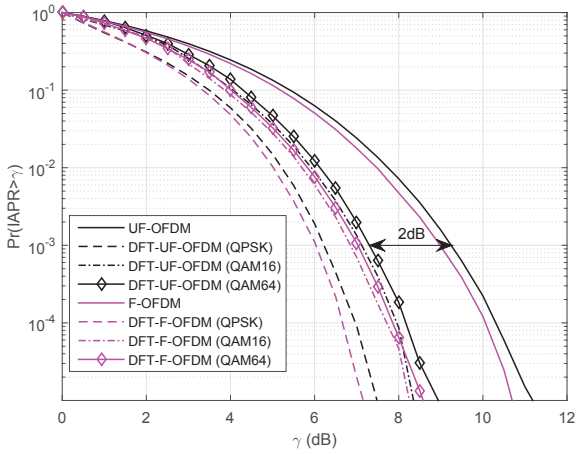

Fig. 7. IAPR performance of the rectangular-based precoded UF-OFDM and F-OFDM schemes for different constellations.

signal obtained at the output of the PA decrease slower than the tails of the spectrum of the signal at its input, which proves that the non-linearity of the PA reduces the spectral efficiency of transmitters based on these modulations. Indeed, as the generated power in the adjacent band is significant, the user of this band may be highly interfered. For this reason, a guard band has to be kept between users to avoid interferences, which may reduce the spectral efficiency.

In addition, even though the UF-OFDM and the F-OFDM PSDs are considerably lower than the OFDM signal at the PA input, they have the same level at the PA output. This is due to their similar level of PAPR. Indeed, having the same signal power level and dynamics makes the PA working at the same operating point. Therefore, the PA behavior, and consequently the PA output spectral shape, are almost the same for both UF-OFDM and OFDM signals.

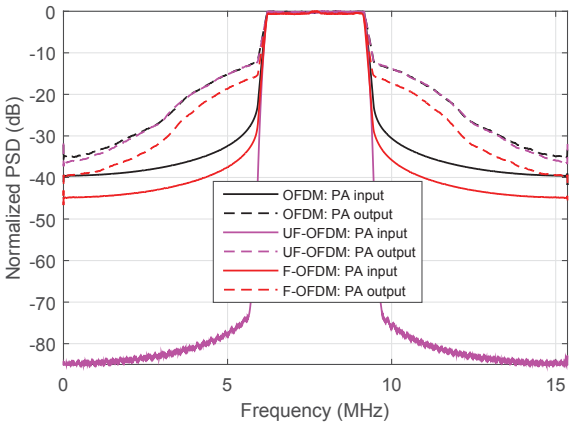

Fig. 8. Normalized PSD-based comparison between the PA output and input signals for OFDM, F-OFDM and UF-OFDM modulations (IBO=5 dB).

In Fig. 9, one can notice that when reducing the PAPR of the PA input signal, the PSD tails of the PA output signal are lower than the case of the original UF-OFDM signal. The different obtained PSD tails level are summarized in TABLE II. As it can be seen from this latter, when the DFT-F-OFDM modulation scheme is used, the PSD tails are lower than the case when the DFT-UF-OFDM modulation scheme is used. This can be explained by the difference between the PAPR and IAPR levels for both schemes. Indeed, as the PAPR level of the DFT-F-OFDM is lower than the DFT-UF-OFDM one, the PA is not driven to the same operation point for the two schemes.

C. Impact on the BER performance

In the Fig. 10, the BER performance of the DFT-UF-OFDM and the DFT-F-OFDM are compared to the UF-OFDM for the 16-QAM and the 64-QAM constellations. As it is shown in this figure, the precoding has no effect on the BER performance in a AWGN channel. Hence, adding a precoding block to the modulation scheme improves the PAPR CCDF, the

ISBN 978-3-8007-4426-8

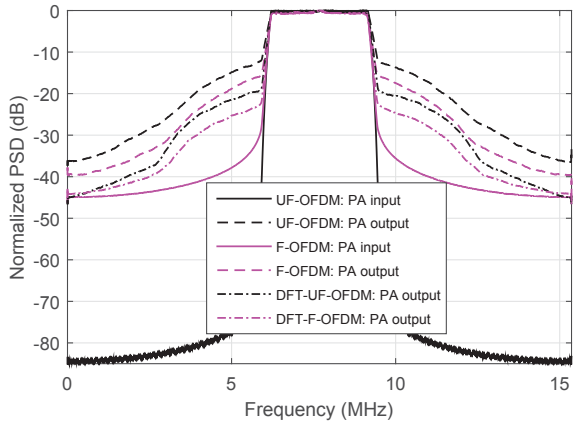

Fig. 9. Normalized PSD-based comparison between the PA output and input signals for the UF-OFDM, the F-OFDM, the DFT-UF-OFDM and the DFT-F-OFDM (IBO=5 dB).

PSD tails and does not impact the BER performance. Indeed, as the precoding is an orthogonal process, it conserves the orthogonality state of the modulation scheme.

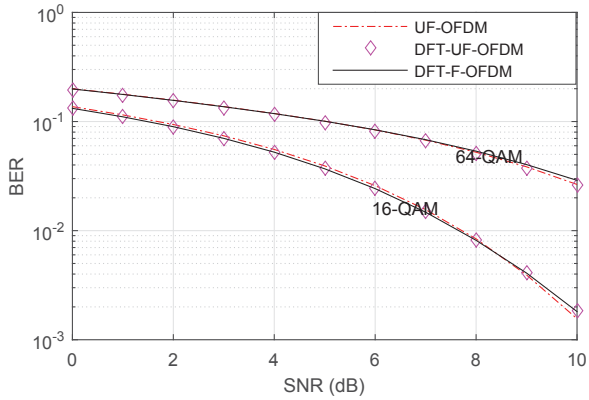

Fig. 10. BER comparison between, the UF-OFDM, the DFT-UF-OFDM and the the DFT-F-OFDM for the 16-QAM and the 64-QAM constellations.

V. Conclusion

In this work, a PAPR reduction technique for the UF-OFDM and the F-OFDM modulation schemes was proposed. This technique has to keep the spectral efficiency and the BER performance of the system. For this reason, a precoding-based PAPR reduction technique was proposed. This technique transforms the F-OFDM signal to a single carrier signal and the UF-OFDM to a multicarrier signal with smaller number of carriers. At the receiver, the received symbols can be decoded without the need of sending any "side information" and consequently without reducing the spectral efficiency. In addition to the PAPR and the PA output PSD tails reductions, this method conserves the BER in an AWGN channel. Further studies will be performed in the upcoming works about their BER performance in a frequency selective channel.

Acknowledgment

This work is funded through the French National Research Agency (ANR) project WONG5 with grant: ANR-15-CE25-0005-03.

References

[1] U. Siddique, H. Tabassum, E. Hossain and D. I. Kim, "Wireless backhauling of 5G small cells: challenges and solution approaches," IEEE Wireless Communications, vol. 22, no. 10, pp. 22-31, 2015.

[2] M. Matthe, D. Zhang, F. Schaich, T. Wild, R. Ahmed and G. Fettweis, "A Reduced Complexity Time-Domain Transmitter for UF-OFDM," IEEE Vehicular Technology Conference (VTC Spring), Nanjing, pp. 1-5, 2016.

[3] S. Cripps, *Advanced techniques in RF power amplifier design*, Artech House, 2002.

[4] A. A. Gorji and R. S. Adve, "Waveform optimization for random-phase radar signals with PAPR constraints," 2014 International Radar Conference, pp. 1-5, 2014.

[5] F. Tosato, M. Sandell and M. Tanahashi, "Tone reservation for PAPR reduction: An optimal approach through sphere encoding," 2016 IEEE International Conference on Communications (ICC), Kuala Lumpur, pp. 1-6, 2016.

[6] W. Wang, M. Hu, Y. Li, H. Zhang, "A low-complexity tone injection scheme based on distortion signals for PAPR reduction in OFDM systems," IEEE Transactions on Broadcasting, no. 06, pp. 1-9, 2016.

[7] J. Mountassir, A. Isar and T. Mountassir, "Precoding techniques in OFDM systems for PAPR reduction," IEEE Mediterranean Electrotechnical Conference, pp. 728-731, 2012.

[8] J. Abdoli, M. Jia and J. Ma, "Filtered OFDM: A new waveform for future wireless systems," International Workshop on Signal Processing Advances in Wireless Communications (SPAWC), pp. 66-70, 2015.

[9] M. Chafii, J. Palicot, R. Gribonval, "Closed-form approximations of the peak-to-average power ratio distribution for multi-carrier modulation and their applications," EURASIP Journal on Advances in Signal Processing, vol. 2014, no. 1, p. 121, 2014.

